International Journal of Multiphase Flow 35 (2009) 977–986

Contents lists available at ScienceDirect

International Journal of Multiphase Flow

journal homepage: www.elsevier.com/locate/ijmulflow

# Experimental study on critical heat flux in bilaterally heated narrow annuli

Y.W. Wu, G.H. Su *, S.Z. Qiu, B.X. Hu

*State Key Laboratory of Multiphase Flow in Power Engineering, Department of Nuclear Science and Technology, Xi'an Jiaotong University, Xi'an City 710049, China*

ARTICLE INFO

*Article history:*
Received 15 January 2009
Received in revised form 18 June 2009
Accepted 9 July 2009
Available online 19 July 2009

*Keywords:*
Narrow annular channel
Critical heat flux
Bilateral heating

ABSTRACT

Critical heat flux (CHF) experiments using deionized water as working fluid have been conducted in a range of pressure from 0.6 to 4.2 MPa, mass flow velocity from 60 to 130 kg/m$^2$ s and wall heat flux from 10 to 90 kW/m$^2$ for vertical narrow annuli with annular gap sizes of 0.95 and 1.5 mm. We found that the CHF, occurring only on the inside tube, or on the outside tube or on both tubes of the annular channel, depends on the heat flux ratio between surfaces of the outside and inside tubes. The CHF, occurring on the surface of the inside tube, reaches the maximum value under the pressure of 2.3 MPa while it occurring on the surface of the outside tube keeps increasing with the increase of the pressure. The CHF, occurring on the inside or outside tubes, increases with the increase of the mass flow velocity and the annular gap size; and decreases with the increase of critical quality and the other tube wall heat flux. Empirical correlations, which agree quite well with the experimental data, have been developed to predict the CHF occurring on surfaces of the inside or outside tubes of the narrow annular channel on the conditions of low pressure and low flow.



## 1. Introduction

In recent years, much attention has been paid to the compact heat exchanger due to its intrinsic superior characteristics of high thermal efficiency, small size, light weight, energy saving etc. and can be used in various industrial progresses, such as cooling of electric device, refrigeration or air conditioning and nuclear engineering. The concentric narrow annular channel is one kind of this heat transfer tube in the compact heat exchanger. It uses dual-tube structure for heat exchange and the gap size between the two tubes is very small, ranging from 0.5 to 2.5 mm. In this narrow channel, due to the fluid's being confined by the narrow gap, flow patterns and heat-exchange mechanisms of the fluid flow are quite different from those in common tubes and the occurrence mechanism of critical heat flux (CHF) is accordingly different. The CHF is one of the important thermal hydraulic parameters limiting the available power in many systems. When CHF occurs, the heat transfer capacity will decrease dramatically and the correspondingly the wall temperature will rise rapidly, even to melt down the heat transfer surface (Wang et al, 2000). In order to realize the optimal design and ensure a high degree of safety in the compact heat exchanger using the narrow annular channel as its heat transfer tube, the CHF characteristics in the narrow annular channel need to be understood clearly.

Extensive studies on the CHF have been performed over the past few decades, especially with the development of nuclear reactor. Most of them concentrated on conventional round tubes or rod bundles on the conditions of high pressure and high mass flow velocity, which are the operating conditions of commercial water-cooled nuclear reactors. However, CHF studies on narrow channels (e.g. narrow rectangular channel, narrow annular channel) are very limited. Previous research on the narrow annular channel is reviewed briefly as follows.

Boiling in a horizontal tube with the annular type of confinement was studied experimentally by Jensen et al. (1976). The dryout heat flux was found to be directly proportional to the clearance and inversely proportional to the length of the annulus. Compared to an open tube, the dryout heat flux is reduced by a factor of ten.

Chang and Yao (1983) investigated the CHF in narrow vertical annuli with closed bottom for various fluids under different pressures and found that the CHF is generally much lower than that in the open pool boiling due to different controlling mechanisms. Based on the experimental data, a semi-empirical correlation for this problem by modifying the flooding model of Wallis (1969) was established.

Mishima and Nishihara (1987) reviewed the previous experiments for water in an annulus, rectangular ducts and a round tube, and found that the effect of channel geometry turns out to be remarkable at intermediate mass flow velocities due to the existence of an unheated wall which causes a non-uniform distribution of liquid film.

El-Genk et al. (1988) performed experiments to measure the CHF for low flow flux of water in vertical annuli under near atmospheric pressure. Results showed that the CHF increases with the increase of the water mass flow velocity or annulus ratio. However,

* Corresponding author. Tel./fax: +86 29 82663401.
*E-mail address:* ghsu@mail.xjtu.edu.cn (G.H. Su).

0301-9322/$ - see front matter © 2009 Elsevier Ltd. All rights reserved.
doi:10.1016/j.ijmultiphaseflow.2009.07.004

the effect of inlet subcooling on CHF is not distinguishable in the smaller annuli (annulus ratios of 1.575 and 1.72) and the largest annulus (annulus ratios of 2.0) when mass flow velocity is less than 140 kg/m$^2$ s. Conversely, in the largest annulus at higher mass flow velocity, the CHF values increases as the inlet water subcooling increases.

Park et al. (1997) assessed existing correlations based on 1156 experimental data and found that there are no correlations which could predict the low-pressure, low-flow CHF satisfactorily.

Doerffer et al. (1997) examined CHF behavior for the annular channel with bilateral heating and compared it with that in tubes and internally heated annuli. It was found that the quality and pressure are identified as the most important parameters to account for differences in CHF between bilaterally and unilaterally heated annuli or tubes. Based on the droplet-diffusion model proposed by Kirillov and Smogalev (1969, 1972), the CHF correlations for internal, external and bilateral heating conditions were developed according to the annuli CHF data of Becker and Letzter (1975).

Monde et al. (1999) proposed that the role of heated equivalent diameter on CHF is important for an annular tube on the conditions of inside or outside single-side heating.

Kim et al. (2000) performed CHF experiments with annular test sections submerged in a pool of saturated water under near atmospheric pressure with the inclination angles from horizontal to vertical positions. The experimental results revealed that the CHF increases with the gap size and the inclination angle.

Stoddard et al. (2002) explored the CHF in thin horizontal annuli and found that the measured CHF values are considerably lower than the expected CHF values for vertical test section configuration.

Kim et al. (2007) examined the effects of mechanical vibrations on CHF under near atmospheric pressure in a vertical annulus tube and found that CHF is increased by mechanical vibration up to 16.4% and vibration amplitude is one of the effective parameters on CHF enhancement.

Lee et al. (2008) investigated the CHF characteristics for a vertical annular channel with one heated rod and four spacer grids for new refrigerant R-134a and concluded the CHF data for annular channel agreed with previously developed correlations for tube reasonably but with a shift of distribution around ±50%.

The CHF correlations for narrow annuli are summarized in Table 1.

As described above, the processes of thermodynamics and fluid dynamics causing the phenomena of CHF in narrow annuli are complex and the physical mechanisms resulting in the CHF phenomenon in narrow annuli have not been understood sufficiently. There are several empirical correlations for predicting the CHF in narrow annuli. However, they are developed mainly based on the CHF data from internal heating annuli and the application ranges of these correlations are restricted. The only correlation (Doerffer et al., 1997) was developed based on the CHF data from bilateral heating annuli under the pressure from 7 to 10 MPa and mass flow velocity from 500 to 4000 kg/m$^2$ s which was applicable to relatively high pressure and high mass flow velocity conditions. Therefore, this work is devoted to improving the understanding of the CHF phenomenon on the conditions of low pressure and low mass flow velocity in narrow annuli, enriching the experimental data base, and providing prediction correlations by performing CHF experiments in vertical narrow annuli with bilateral heating.

## 2. Experiments

There are two mechanisms for the onset of CHF: one is departure from nucleate boiling, and the other is dryout. From an engineering point of view, the CHF caused by the latter mechanism is of particular importance since annular flow is one of the most common flow patterns in gas–liquid two-phase flow, and especially it is the main flow pattern of the flow boiling in vertical narrow annuli (Park et al, 1997; Inoue and Lee, 1999; Chun et al, 1999). Therefore, the present study performs CHF experiments caused by the liquid film dryout.

### 2.1. Experimental loop

The dryout experimental test loop is shown schematically in Fig. 1. It consists of two main loops, namely, the primary and secondary loops. The secondary loop, which is connected to the primary one through a condenser, is used to condense the fluid in the primary loop and is not shown in detail in Fig. 1. The fluid circulated by the pump in the primary loop flows through the preheater, the flow meter, and then it is fed into the test section and flows into the condenser. The mass flow velocity of the test section can be regulated by adjusting the gate opening of the bypass valve. The system pressure can be regulated by adjusting charge of nitrogen through the nitrogen charging line. The more precise mass flow velocity and system pressure can be further adjusted by the needle valve at the upstream of the flow meter section and the power of the heater in the pressurizer, respectively.

### 2.2. Test sections

Two test sections were used in this study. As shown in Fig. 2, they are composed of two concentric straight stainless steel tubes with the fluid flowing through the annular space between the two tubes. They have the following geometrical parameters: 10 mm i.d. and 2 mm thickness of outside tube, 8.1 and 7 mm o.d. and 1 mm thickness of inside tube. Thus the corresponding annular gap sizes of the two test sections are 0.95 and 1.5 mm respectively. The inside and outside tubes of the test section were heated by two low voltage and high current direct currents respectively and the heat fluxes of inside and outside tubes can be adjusted respectively. NiCr–NiSi thermocouples with $\Phi$0.5 mm were spot-welded on the outer surface of fifteen cross-sections at each interval of 25 mm along the axial direction of the outside tube. In each horizontal cross-section, four thermocouples were arranged on the outside tube with 90° apart and the average value of them was regarded as the outer wall temperature of the outside tube in this section. For thermocouples cannot be spot-welded directly on the surface of the inside tube as on the surface of the outside tube, and the following method was adopted to measure temperatures on the surface of the inside tube. Firstly, fifteen NiCr–NiSi armoured thermocouples with $\Phi$0.5 mm were arranged on the work table according to the thermocouples distribution of the outside tube and bundled up one by one. The thermocouples were wrapped by a thin flexible electrical insulation mica belt to keep electrical insulation between the thermocouples and the inside tube, and then a thin, long thermocouple assembly was formed. Finally, the thermocouple assembly was inserted into the inside tube carefully to make the locations of the thermocouples be in one-to-one correspondence with that of the thermocouples on the outside tube. The space between the inside tube and the thermocouple assembly was filled with Boron Nitride(BN) powder, which is of good electrical insulation and high thermal conductivity, to improve each other's electrical insulation and thermal conduction. The good electrical insulation can avoid the electric conduction between the thermocouple assembly and the inside tube which is connected a DC current power. The high thermal conduction would make the experimental condition reach a steady condition sooner when the power level is raised again. In the experiment, there is no internal heat source in the inside space of the inside tube, and

**Table 1**
Summary of CHF correlations in narrow annuli

| Authors | Correlations | Conditions for studying |
|---|---|---|
| Chang and Yao (1983) | $\frac{q_{CHF}L}{h_{fg}\rho_f sV}\left(1+\frac{\rho_f}{\rho_g}\right)^2 = 0.38$<br>where $L$ is the length of annulus, $s$ is the annular gap size, $V=\left[\frac{gD(\rho_f-\rho_g)}{\rho_f}\right]^{1/2}$ $D$ is the average diameter of the annulus and $h_{fg}$ is the latent heat of vaporization | Narrow vertical annuli with closed bottoms<br>Internal heating<br>Working fluid: Fron-113, acetone and water<br>$s$ : 0.32, 0.80 and 2.58 mm<br>$D_i$ : 25.4 mm<br>$D_o$ : 26.04, 27.00 and 30.56 mm<br>$G$: 0 kg/m$^2$ s<br>$P$: 0.1 MPa |
| El-Genk et al. (1988) | $q^*\left(\frac{A_h}{A}\right) = 1.65\left[\frac{L}{D_{he}}\right]^{0.2}\left[0.933+0.212\frac{G^*\Delta h_i}{h_{fg}}\right]$ for both the slug-churn and the churn–annular flow transitions<br>$q^*(\frac{A_h}{A}) = 0.85N_{\mu f}^{-0.2}+1.045\frac{\Delta h_i}{h_{fg}}G^*$ for the annular–annular mist flow transition<br>where $q^* = q_{CHF}/(h_{fg}A_h\sqrt{\lambda\rho_v g\Delta\rho})$, $G^* = G/\sqrt{\lambda\rho_v g\Delta\rho}$, $\lambda=\sqrt{\sigma/(g\Delta\rho)}$, $N_\mu f = \mu_f/(\rho_f\sigma\sqrt{\sigma/(g\Delta\rho)})^{0.5}$, $L$ is the length of heated section, $D_{he}$ is the equivalent diameter based on heated perimeter and $\Delta h_i$ is the inlet subcooling enthalpy | Narrow vertical annuli<br>Internal heating<br>Working fluid: water<br>Inlet subcooling: 182–312 kJ/kg<br>s: 3.65, 4.55 and 6.35 mm<br>$D_i$ : 12.7 mm<br>$D_o$ : 20.0, 21.8 and 25.4 mm<br>$G$: 0—260 kg/m$^2$ s<br>$P$: 0.118 MPa |
| Doerffer et al. (1997) | $q_{CHF,i} = \frac{r_i+r_o}{r_i}\times\frac{K_a h_{fg}\rho_g}{x_{n1}}\times(x_n-\phi_{oi}-x_c)$ for the CHF in internally heated annulus<br>$q_{CHF,i} = \frac{r_i+r_o}{r_i}\times\frac{K_a h_{fg}\rho_g}{x_{n1}}\times(x_n-\phi_o-x_c)-\frac{r_o}{r_i}q''_o$ for the CHF on inner surface during bilateral heating<br>$q_{CHF,o} = \frac{r_i+r_o}{r_o}\times\frac{K_a h_{fg}\rho_g}{x_{n1}}\times(x_n-\phi_{ie}-x_c)$ for the CHF in externally heated annulus<br>$q_{CHF,o} = \frac{r_i+r_o}{r_o}\times\frac{K_a h_{fg}\rho_g}{x_{n1}}\times(x_n-\phi_i-x_c)-\frac{r_i}{r_o}q''_i$ for the CHF on outer surface during bilateral heating<br>where $K_a = 0.15869+3.5917\times10^{-5}\times P^{0.25}-0.047\times P^{0.5}+1.7591\times P^{-2}$<br>$x_n = x_c\frac{K_a h_{fg}\rho_g(r_i+r_o)}{K_a h_{fg}\rho_g(r_i+r_o)-(r_i q_i+r_o q_o)}$ and $x_{n1}=x_n$ | Narrow vertical annuli<br>Bilateral heating<br>Working fluid: water<br>Inlet quality: -0.03 to -0.06<br>$s$: 4.65 mm<br>$D_i$ : 12.0 mm<br>$D_o$ : 21.3 mm<br>$G$: 500—4000 kg/m$^2$ s<br>$P$: 7—10 MPa |
| Monde et al. (1999) | $\frac{q_{CHF}/\rho_g h_{fg}}{\sqrt[4]{\sigma g(\rho_f-\rho_g)/\rho_g^2}} = \frac{0.16}{1+0.075(L/D_{he})}$ for $s=1$ mm<br>$\frac{q_{CHF}/\rho_g h_{fg}}{\sqrt[4]{\sigma g(\rho_f-\rho_g)/\rho_g^2}} = \frac{0.16}{1+0.025(L/D)}$ for $s\geqslant 3$ mm<br>where $D$ is the inner diameter of outer tube, $D_{he}$ is the heated equivalent diameter and $L$ is the length of heated tube | Narrow vertical annuli<br>External heating<br>Working fluid: water<br>$s$: 1, 2, 3 mm; 1, 2, 3, 4 mm and 1, 2 mm<br>$D_i$: 3, 5, 7 mm; 4, 6, 8, 10 mm and 13, 15 mm<br>$D_o$: 9 mm; 12 mm and 17 mm<br>$P$: 0.1 MPa |
| Kim et al. (2000) | $q_{CHF} = \rho_g h_{fg}\left(\frac{s}{L}\right)\left[\frac{gL\sin\theta[(\rho_f/\rho_g)-2]}{1+fL/2s}\right]^{1/2}$ where $f$ is the friction factor, $0.0041\times s^{(3.66\log s-0.94)}$ | Narrow annuli with inclination angles from horizontal to vertical positions<br>External heating<br>Working fluid: water<br>$s$: 0.5, 1.5, 3.0 and 3.5 mm<br>$D_i$: 19 mm<br>$D_o$: 20, 22, 25 and 26 mm<br>$P$: 0.1 MPa |
| Chun et al. (2001a) | $q_{CHF} = C_w^2\left(\frac{D_{he}}{L_{cB}}\right)^{1.396}h_{fg}(gD_h\rho_g\Delta\rho)^{1/2}\times\left[1+\left(\frac{\rho_g}{\rho_f}\right)^{1/4}\right]^{-2}$<br>where $C_w^2 = 1.22\left(\frac{L_B}{D_{he}}\right)^{0.12}\left(\frac{\rho_g}{\rho_f}\right)^{-0.032}\times(1+0.055B_o-4.08\times10^{-3}B_o^2)$, $L_{CB}$ is the length from the onset of saturated boiling to the location of CHF occurrence, $D_h$ is the hydraulic equivalent diameter, $L_B$is the boiling length in the heated section and $B_o$ is the Bond number, $D_h(g\Delta\rho/\sigma)^{1/2}$ | Narrow vertical annuli<br>Internal heating |

(*continued on next page*)

**Table 1** (*continued*)

| Authors | Correlations | Conditions for studying |
|---|---|---|
| | | Working fluid: water<br>$s$: 4.93 mm<br>$D_i$: 9.54 mm<br>$D_o$: 19.4 mm<br>$G$: 0 kg/m$^2$ s<br>$P$: 0.52–14.96 MPa |
| Lee et al. (2008) | $q_{CHF} = 132.0687P^{-0.0982}G^{-0.0505}X_C^{-0.4667}$<br>$q_{CHF} = 6.713P^{-0.173}G^{0.4143}\Delta h_i^{0.3148}$<br>where $X_C$ is the critical quality. | Vertical annular channel with one heated rod and four spacer grids<br>Internal heating<br>Working fluid: R-134a<br>Inlet temperature: 25–40 °C<br>$s$: 0.32, 0.80 and 2.58 mm<br>$D_i$ : 9.5 mm<br>Rectangular flow channel: 19×19 mm$^2$<br>($D_h$ = 10.97 mm, $D_{he}$ = 38.90 mm)<br>$G$: 100–600 kg/m$^2$ s<br>$P$: 1.16, 1.3, 1.6 and 2 MPa |

two ends of the test section were covered by heat insulator and the axial heat conduction can be neglected. Theoretically, on steady experimental conditions, whatever material is filled in the space between the inside tube and the thermocouple assembly, the temperature distribution along the inside vertical space is equal to the inner wall surface temperature distribution along the inside tube. Practically, the condition that the one-digit displays of wall temperatures on the data acquisition system are not change after the power level is raised is regard as a steady experimental condition. The error has been considered in the uncertainty analysis of the wall temperatures.

There was a heater block in the inlet region of the test section. It was a red copper cylinder with 108 mm in length and 100 mm in diameter. Ten holes of 16 mm in diameter and 95 mm in depth were drilled along the circumference of 70 mm in diameter equidistantly. And 10 heating rods of 16 mm in diameter and 115 mm in length were put into these holes. The effective heating length was about 89 mm and the heating power of each rod was 400 W. Furthermore, there was a hole with the diameter of 14.5 mm at the center of the cylinder which can fit the outer diameter of the outside tube and its gap size is 0.25 mm. The molten tin (Sn) was put into this gap to get better heat conduction between the cylinder and the outside tube. A corkscrew groove with both the breadth and depth of 3 mm was lathed around the heater block. Besides, a heater wire of 3 mm in diameter and 6.5 m in length was put into the groove and the heating power was 3.5 kW. Two holes with 1.2 mm in diameter were drilled symmetrically at circles of 19.5 and 42.5 mm in diameter to measure the quantity of power from the heater block to the outside tube, and two NiCr–NiSi armoured thermocouples ($\Phi$1 mm) were inserted into the holes. The quantity of power from the heater block to the outside tube can be calculated according to the measured temperatures.

To thermally insulate the test section from the environment, the whole test section was firstly covered by silicon–aluminium glass fiber of 120 mm in thickness, a wire heater of 3 kW in maximum power winded the outside of this heat insulator to compensate for the heat loss of the test section, and then another silicon–aluminium glass fiber of 50 mm in thickness wrapped the whole test section. Two thermocouples were located in different places of the inner silicon–aluminium glass fiber along radial direction. Then good heat insulation of the test section could be realized by controlling the power of the wire heater and making the measured values by the two thermocouples equal to each other as possible.

### 2.3. Test conduct

Experiments have been performed with the upward flow of deionized water on conditions of different pressure, mass flow

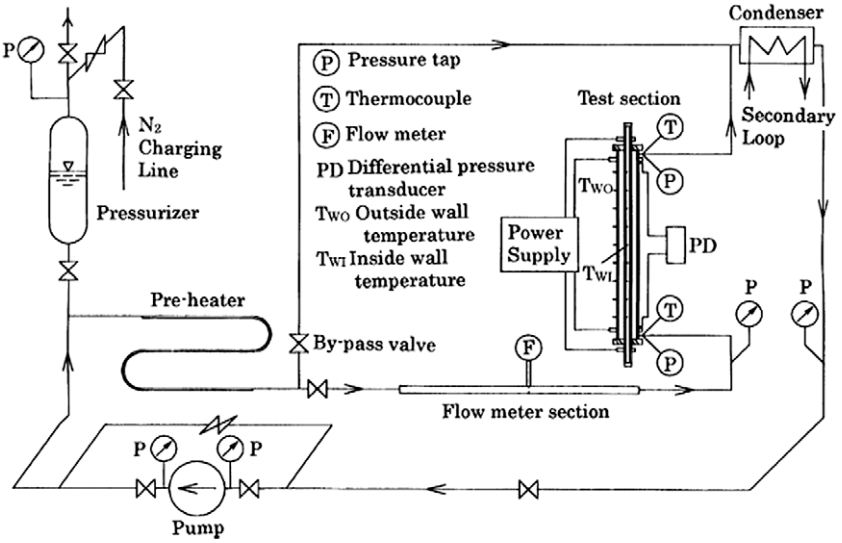


**Fig. 1.** Schematic diagram of experimental apparatus.

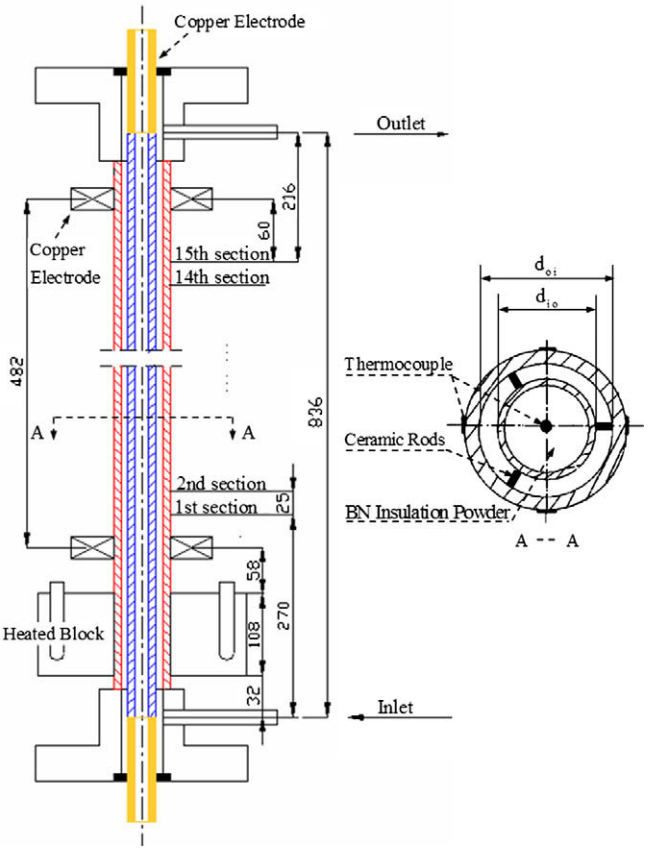


**Fig. 2.** Schematic diagram of the test section.

velocity and wall heat flux. Ranges of parameters tested in the experiment are summarized in Table 2.

To reduce the possible non-condensable gas content, the water in the loop was circulated and boiled for about half an hour before the operation of experiments. And then, the inlet water temperature, mass flow velocity and pressure were adjusted to the demanded values. After those setting, the electric powers were connected to the test section and increased step by step until the occurrence of CHF. The increment of the heat fluxes between power levels was kept sufficiently small and the measured parameters were stabilized before the power level was raised again to ensure steady experimental conditions.

## 3. Data reduction

As mentioned in Section 2.2, the outer surface temperatures of the outside tube were measured by $\Phi$0.5 mm thermocouples spot-welded on the outer surface and the inner surface temperatures of the inside tube were measured by thermocouples inserted into the inside tube. Therefore, the outer surface temperature of the outside tube $T_{woo}$ and the inner surface temperature of the inside tube $T_{wii}$ can be directly measured by thermocouples. However, for experimental data reduction, we need the inner surface temperature of the outside tube $T_{woi}$ and the outer surface temperature of the inside tube $T_{wio}$. Thus, for this purpose, a progress of conduction in a column with average heat sources is evaluated and the final results can be written as

$$T_{woi} = T_{woo} - \left(\frac{q_o}{k_w}\right)\left(\frac{d_{oi}}{d_{oo}^2 - d_{oi}^2}\right)\left(\frac{d_{oo}}{2}\right)^2 \times \left[2\ln\left(\frac{d_{oo}}{d_{oi}}\right) + \left(\frac{d_{oi}}{d_{oo}}\right)^2 - 1\right] \quad (1)$$

$$T_{wio} = T_{wii} - \left(\frac{q_i}{k_w}\right)\left(\frac{d_{io}}{d_{io}^2 - d_{ii}^2}\right)\left(\frac{d_{ii}}{2}\right)^2 \times \left[\left(\frac{d_{io}}{d_{ii}}\right)^2 - 2\ln\left(\frac{d_{io}}{d_{ii}}\right) - 1\right] \quad (2)$$

where $k_w$ is the tube wall thermal conductivity, $q_o$ and $q_i$ are the heat flux of the outside and inside tubes, $d_{oo}$ and $d_{oi}$ are the outer and inner diameters of the outside tube, $d_{io}$ and $d_{ii}$ are the outer and inner diameters of the inside tube.

In the flow boiling heat transfer region, the temperature of the fluid is kept on the saturated level and the wall temperature is also kept at nearly a constant value. When CHF occurs, due to the poor heat-transferring capability of the vapor, the wall temperature

**Table 2**
Experimental conditions.

| Parameters | Range |
|---|---|
| System pressure, $P$ (MPa) | 0.6–4.2 |
| Mass flow velocity, $G$ (kg/m$^2$s) | 60–130 |
| Heat flux of outside tube, $q_o$ (kW/m$^2$) | 10–90 |
| Heat flux of inside tube, $q_i$ (kW/m$^2$) | 10–60 |
| Critical quality, $X_C$ | 0.45–0.95 |

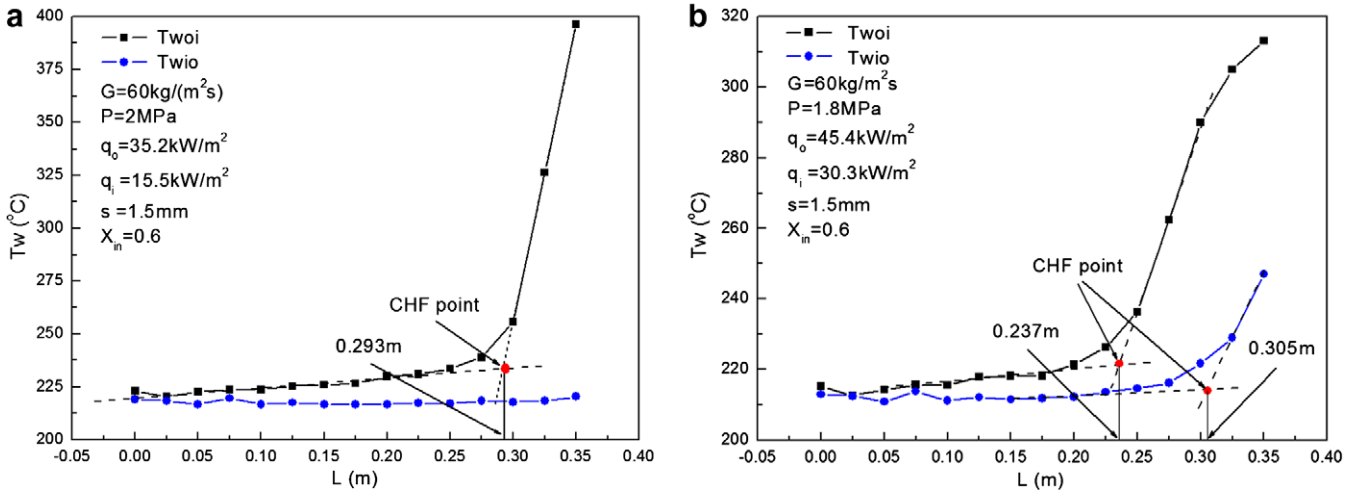


**Fig. 3.** Determination of the location of CHF points: (a) CHF occurring on outer annulus surface and (b) CHF occurring on inner annulus surface.

**Table 3**
Summary of the uncertainty analysis.

| Parameters | Uncertainty (%) |
|---|---|
| *Annular channel geometry* | |
| Length and diameter, $L$ and $d$ | ±0.25 |
| Area, $A$ | ±0.5 |
| *Parameter measurement* | |
| Wall temperature, $T$ | ±0.75 |
| Water temperature, $t$ | ±0.75 |
| System pressure, $P$ | ±0.25 |
| Mass flow velocity, $G$ | ±0.25 |
| Voltage, $U$ | ±0.5 |
| Current, $I$ | ±0.1 |
| Data acquisition system | ±0.02 |
| *Parameter calculation* | |
| Imposed heat flux, $q$ | ±3 |
| Critical quality, $X_C$ | ±5 |

rises rapidly. Thus, in this study, the CHF condition can be observed with the rapid rise of the tube wall temperature monitored by the thermocouples arranged in the test section and the location of the CHF can be determined by the crossing point of two tangent curves according to the rapid change of the tube wall temperature as shown in Fig. 3, where the horizontal coordinate $L$ is the axial length of the channel which adopts the location of the first measuring section as the zero point and the vertical coordinate $T_w$ is the tube wall temperature. It is easy to see that the CHF occurs only on the outside tube and the axial length of CHF point is 0.293 m from Fig. 3(a) while the CHFs occur on both inside and outside tubes and the axial lengths of CHF points are 0.237 and 0.305 m from Fig. 3(b). By the location of CHF point, critical quality $X_C$ can be calculated by the following equation:

$$X_C = \frac{C_p t_{f,in} + (L_c/L) \times (q_i A_i + q_o A_o)/(GA_f) - h_f}{h_{fg}} \quad (3)$$

where $C_p$ is the specific heat capacity, $t_{f,in}$ , which can be calculated by the inlet water temperature of the test section and the imposed heat flux of the heater block, is the water temperature of the first measuring section of the test section and then the inlet quality $X_{in}$ can be obtained by $X_{in} = \frac{C_p t_{f,in} - h_f}{h_{fg}}$, $L_c$ is the distance between the locations of the first measuring section of the test section and the CHF point, $A_i$ and $A_o$ are the heating area of the inside and outside tubes respectively, $G$ is the mass flow velocity, $A_f$ is the flow area of the test section, $h_f$ is the specific enthalpy of saturated water and $h_{fg}$ is the latent heat of vaporization.

In this study, all the measuring devices were calibrated by the authoritative institutes. Uncertainties of the mass flow velocity, the system pressure, the heat fluxes of the two heated surfaces, the critical quality etc. are estimated according to the procedures proposed by Kline and McClintock (1953) for the propagation of errors in physical measurement. The results of the uncertainty analysis are summarized in Table 3.

## 4. Results and discussion

### 4.1. Characteristics of the occurrence of CHF

It is easy to see from Fig. 3 that the CHF occurred only on outer annulus surface as shown in Fig. 3(a) while the CHF occurred simultaneously on both annulus surfaces as shown in Fig. 3(b). The CHF sometimes occurs only on outer annulus surface, sometimes occurs only on inner annulus surface and sometimes occurs on both annulus surfaces. The main reason is the difference of heat fluxes between the inside and outside tubes which may lead to the differences of the liquid film thickness, deposition and entrainment

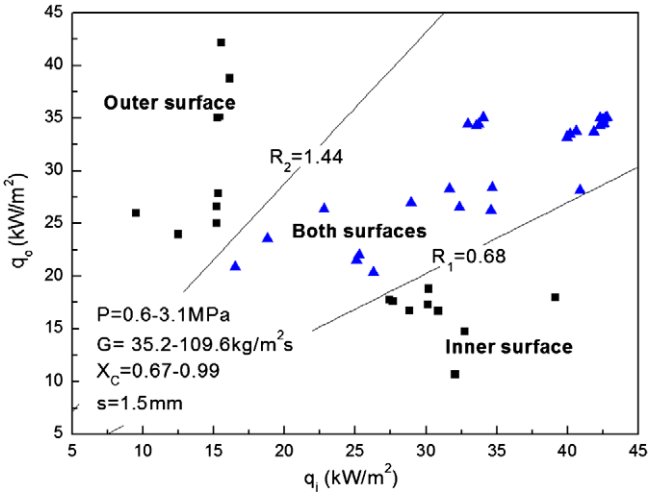


**Fig. 4.** Criterion of the appearance of CHF.

on the two surfaces. The heat flux ratio $R$ between the outside and inside tubes surfaces is hereby defined to examine the effects of the heat fluxes on CHF. The larger $R$ representing the relatively high outside tube heat flux makes the evaporation capability on the outside tube higher and the deposition on the outside tube decrease. Correspondingly, the CHF occurs preferentially on the outside tube. On the contrary, the smaller $R$ means that the CHF occurs preferentially on the inside tube. When $R$ is of medium value, CHF may occur simultaneously on both inside and outside tubes. It can be concluded from Fig. 4.

(1) When $0<R<R_1$, CHF occurs only on inside tube.
(2) When $R_1<R<R_2$, CHF occurs simultaneously on both tubes.
(3) When $R>R_2$, CHF occurs only on outside tube.

$R_1$ is equal to 0.68 and $R_2$ is equal to 1.44, which are fitted for the system pressure of 0.6–3.1 MPa, mass flow velocity of 35.2–109.6 kg/m$^2$ s, critical quality of 0.67–0.99 and annular gap size of 1.5 mm.

In the experiment, it is also found that the value of CHF occurring on the inside tube is less than that of CHF occurring on the outside tube on the same conditions of system pressure, mass flow velocity, inlet quality and the other side heat flux. In other words, the CHF is more likely to occur on the inside tube than on the outside one. There are several reasons for this phenomenon: (1) The shearing force of the inside tube acting on fluid is greater than that of the outside tube in annular flow(Doerffer et al., 1997). Thus, the film thickness on the inside tube is less than the one on the outside tube; (2) The deposition rate on the inside tube is less than that on the outside tube due to the larger view factor (Saito et al., 1978; Doerffer et al., 1997). Compared with the film thickness and the deposition rate, the entrainment rate, which is higher on the outside tube, is low and can be negligible. Thus, the occurrence of CHF on the inside tube needs less power and its corresponding CHF is less than that on the outside tube on the same experimental conditions.

### 4.2. The effect of the pressure on CHF

The CHF of internally heated vertical annulus with the fluid velocity ranging from 550 to 650 kg/m$^2$ s increases rapidly with the increase of pressure, and reaches a maximum value under the pressure of 2–3 MPa and then decreases slowly with the increase of pressure (Chun et al, 2001b). The similar experiments

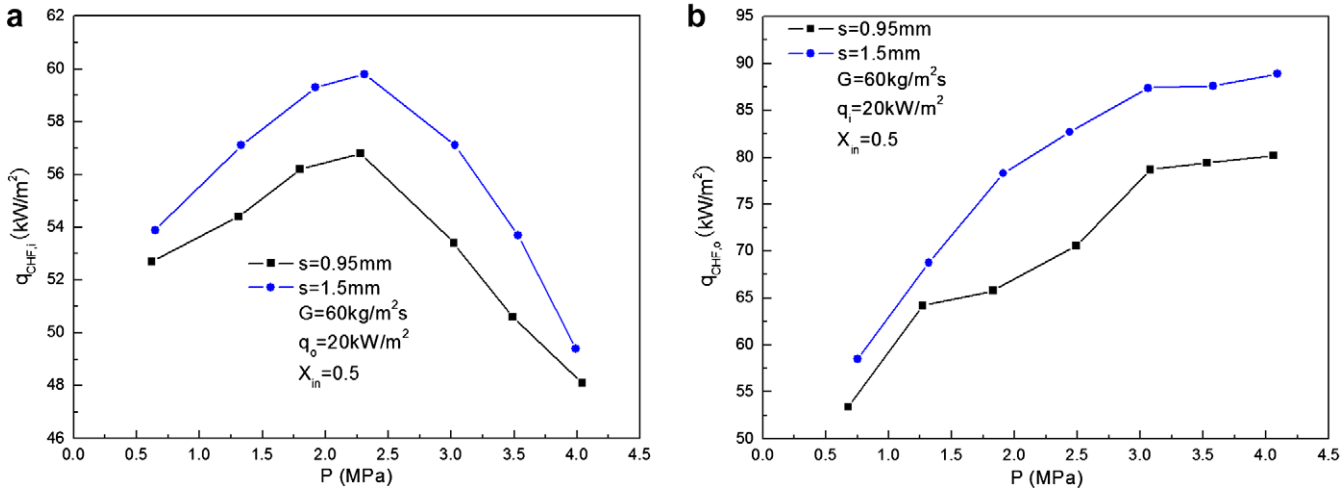


**Fig. 5.** Effect of pressure on CHF: (a) CHF occurring on the surface of the inside tube and (b) CHF occurring on the surface of the outside tube.

were conducted with the pressure ranging from 0.6 to 4.2 MPa in this study and the variation of the CHF with the pressure was shown in Fig. 5(a) and (b) on the condition of mass flow velocity of 60 kg/m$^2$ s, inlet quality of 0.5 and annular gap size of 1.5 mm. Fig. 5(a) shows that the CHF on the inside tube reaches the maximum value under the pressure of about 2.3 MPa for $q_o$ = 20 kW/m$^2$ and this conclusion is consistent with the results of the former research (Chun et al., 2001b). Fig. 5(b) shows that the CHF on the outside tube increases with the increase of the pressure when $q_i$ = 20 kW/m$^2$. This phenomenon may be explained by the following reasons. In annular flow, CHF occurs when the liquid film is dried out by evaporation and entrainment. Evaporation rate increases as pressure increases due to the lower latent heat of vaporization under a higher pressure. Entrainment rate is influenced by the disturbances waves on the interface of liquid film which is determined by slip ratio. If the slip ratio, which is an increasing function of steam-to-water specific volume ratio, is higher, the effect of entrainment is stronger. It is known that steam-to-water specific volume ratio decreases as pressure increases. Therefore, entrainment rate decreases with the increase of pressure. Thus, by these two converse effects, the parametric trends of pressure can be explained. On the conditions of lower pressure, the effect of entrainment plays the dominant role compared with that of evaporation and the CHF increases with the increase of pressure. With the further increase of pressure, the effect of evaporation becomes more and more obvious and then the CHF decreases as pressure increases. On the present experimental conditions, the demarcation pressure for the two effects is about 2.3 MPa for the CHF occurring on the inside tube and it is larger than 4.2 MPa for the CHF occurring on the outside tube. The more precise demarcation pressure for the CHF occurring on the outside tube can be determined by the further experimental studies with wider range of pressure.

### 4.3. The effect of the mass flow velocity on CHF

Much research has been done which is only applied to investigating the mass flow velocity on CHF in internally heated annuli and found that the CHF monotonically increased with the increase of mass flow velocity remarkably (Chun et al., 2001a; Roger et al., 1982; El-Genk et al., 1988; El-Genk and Rao, 1991). In this study, the variation of the CHF with mass flow velocity is shown in Fig. 6. On the condition of a fixed inlet quality and pressure, the CHF occurring on the outside tube increases with the increase of mass flow velocity remarkably. However, the CHF occurring on the inside tube increases with the increase of mass flow velocity slightly and keeps at nearly a constant value with the change of mass flow velocity. This means that the CHF occurring on the inside tube is not influenced significantly by mass flow velocity

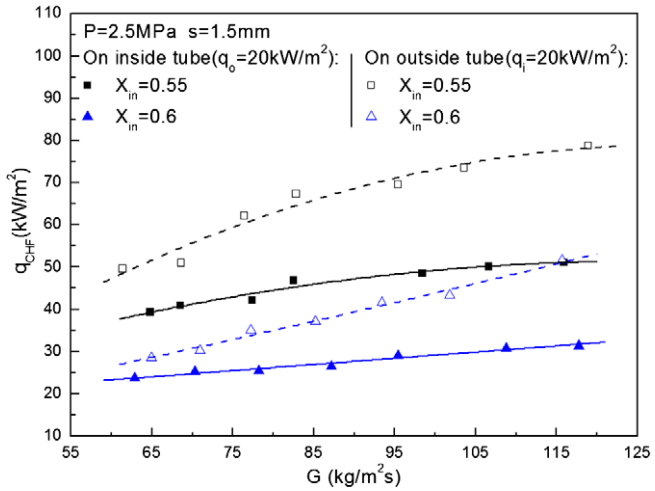


**Fig. 6.** Effect of mass flow velocity on CHF.

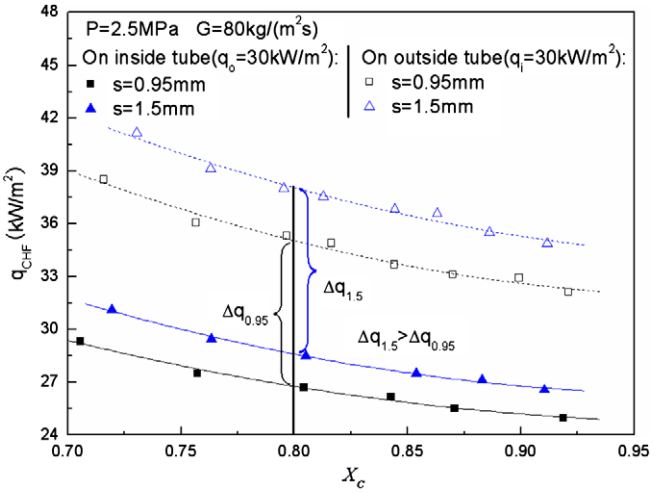


**Fig. 7.** Effects of critical quality, geometrical structure and gap size on CHF.

and it is different from that of the internally-heated annular channel as mentioned above. The effects of deposition and entrainment rates on both sides of tubes increase with the increase of mass flow velocity. These effects on the inside tube are compatible and almost are compensated for each other. Thus, unlike the effect of the mass flow velocity on the CHF for the internally-heated annular channel, the CHF occurring on the inside tube increases with the increase of mass flow velocity slightly. However, the effect of deposition is more intensive than that of entrainment on the CHF occurring on the outside tube of the annular channel with bilateral heating. Thus, the CHF occurring on the outside tube increases with the increase of mass flow velocity remarkably.

### 4.4. The effect of the critical quality on CHF

The critical quality is an important characteristic parameter for dryout point and is related to the total power of the test section. In an annular channel, the heat can be transferred to fluid through both of the inside and outside tubes. The heat fluxes on the inside and outside tubes will determine the power proportions on the inside or outside tubes and they will affect the location of dryout point as described in Section 4.1. It is known that the location of dryout point varies when the heat flux on the dryout tube is adjusted with the other side tube heat flux fixed. When the heat flux on the dryout tube increases, the disturbances waves on the interface of liquid film of this tube get stronger, and the evaporation and entrainment rates increase. Thus, the distance between the inlet of annular channel and the location of dryout point decreases and thus the critical quality decreases. In addition, the contribution of the other side tube to the critical quality also decreases which causes the further decrease of the critical quality. Therefore, as shown in Fig. 7, the CHF decreases with the increase of the critical quality.

### 4.5. The effect of the geometrical structure of annular channel on CHF

Compared with the round tube, the annular channel owns two heating wall surfaces, namely, inside and outside tubes which will result in the unbalance and asymmetry of heating and fluid flow between both sides of tubes. Knudsen and Katz (1958) pointed out that in single-phase flow, whether in the laminar or turbulent flow regions, the shearing force of outside tube acting on fluid is less than that of inside tube. This is also assumed to be true in two-phase annular flow at the vapor–liquid films interfaces (Knudsen and Katz, 1958; Su et al., 2003a,b). In addition, the shearing forces of inside and outside tubes are close to each other when the outer diameter of the inside tube $D_i$ approaches the inner diameter of the outside tube $D_o$. Thus, they proposed that the liquid film thickness on the outside tube was thicker than that on the inside tube at the onset of annular flow and the dryout of the liquid film on the inside tube surface needs less heat than on the outside tube. That is to say, the value of CHF on the inside tube is smaller than that on the outside tube on the condition of a fixed heat flux on the other side. The difference between $D_i$ and $D_o$ is large for $s = 1.5$ mm compared with $s = 0.95$ mm and it leads to the larger difference of shearing force between the inside and outside tubes. Thus, the difference between $q_{CHF,i}$ and $q_{CHF,O}$ for $s = 1.5$ mm is larger than that for $s = 0.95$ mm as shown in Fig. 7: $\Delta q_{1.5}$ is larger than $\Delta q_{0.95}$. Therefore, if the annular gap size is small, that is, $D_i$ approaches $D_o$, the difference between $q_{CHF,i}$ and $q_{CHF,O}$ is smaller.

### 4.6. The effect of the gap size on CHF

In the pre-dryout annular flow region, the fluid flow consists of three components: the liquid film, the high-speed gas flow and the entrained liquid droplets. Parameters including evaporation of the liquid film, deposition of droplets and entrainment on the surface

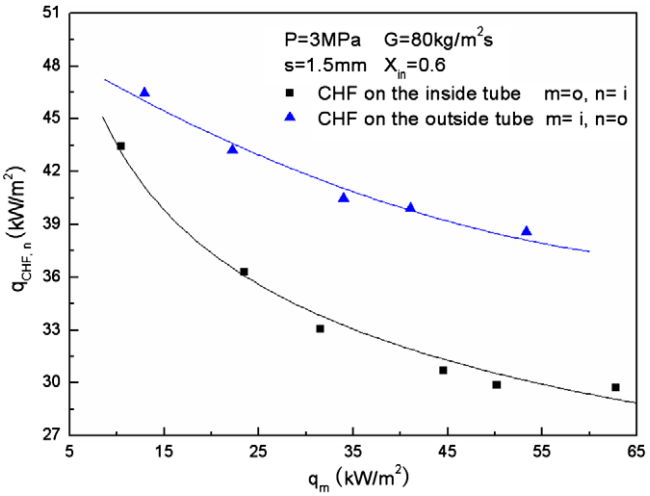


**Fig. 8.** Effect of the other side wall heat flux on CHF.

of the liquid film determine the location of dryout and the corresponding CHF. Under the same conditions, entrainment rate decreases with the increase of the gap size while deposition rate of droplets increases with the increase of gap size. As shown in Fig. 7, when dryout occurs in a narrower annular gap, due to the lower entrainment rate and the higher deposition rate, the liquid film is thicker and the corresponding CHF is larger.

### 4.7. The effect of the different wall heat flux of each side tube on CHF

The fluid can be heated by DC current power on each side of the annular channel. The different heat fluxes on each surface contribute much to the location of dryout and the corresponding CHF. The heat flux determines the evaporation rate of liquid film and it also has a great effect on the deposition rate of droplets for it makes the vapor flow normal to the heated wall. As shown in Fig. 8, on the condition of the same pressure and mass flow velocity, for both of the two sides, the evaporation rate is increased and the liquid film dries out sooner with the increase of the other wall heat flux, which leads to lower CHF. The CHF on the inside tube decreases more quickly with the remarkable increase of heat flux than on the outside tube. For the heated area of outside tube is larger than that of inside tube, and the fluid gets more heat by the same other wall heat flux when CHF occurs on the inside tube.

## 5. Empirical correlation of CHF

As described by Lee et al. (2008), the CHF in forced convective boiling, generally, is a function of the channel geometry, flow conditions and heat flux distributions (uniform or non-uniform heating conditions). For the parametric trends of the CHF in flow boiling of the case where the water is injected into the bottom of an evenly heated, vertical annular channel with bilateral heating, the CHF is a function of seven independent variables, that is, system pressure $P$, heated length $L$, mass flow velocity $G$, inlet specific enthalpy $\Delta h_{in}$, inner diameter of outside tube $D_o$, outer diameter of inside tube $D_i$ and wall heat flux of the other side $q$. This relationship represents the inlet conditions concept, and inlet temperature $t_{in}$ or inlet quality $X_{in}$ can be used instead of inlet enthalpy. In the exit conditions concept, outlet quality $X_{out}$ is used instead of inlet enthalpy. Outlet quality and inlet enthalpy are related to each other via the heat balance equation.

Generally, for the prediction of the CHF, it is common to adopt the local-condition hypothesis that neglects the length effect on

the CHF. The critical quality (local quality at CHF point), $X_C$, is used instead of outlet quality, $X_{out}$, for it is possible to generalize the relationship even for the non-uniform axial heat flux distributions. On the condition of a fixed heated length and evenly heating of the narrow annular channel with bilateral heating, CHF is the following type of function:

$$q_c = f(G, P, X_C, D_i, D_o, q) \tag{4}$$

Therefore, here, the local-condition concept is adopted and the relationships of CHF are correlated with the pressure, mass flow velocity, critical quality, channel geometry and wall heat flux on the other side tube.

The following dimensionless parameters are introduced to develop the correlation with the above influencing factors fully considered. The dimensionless critical heat flux is given by $q_c^* = q_c/\left(h_{fg}\sqrt{\lambda\rho_g g\Delta\rho}\right)$ and the dimensionless mass flow velocity is given by $G^* = G/\sqrt{\lambda\rho_g g\Delta\rho}$ where $h_{fg}$ is the latent heat of evaporation, kJ/kg, $\lambda$ is the length scale of Taylor instability and defined by $\lambda = \sqrt{\sigma/g\Delta\rho}, m, \rho_g$ is the saturated vapor density, kg/m$^3$, $g$ is the acceleration of gravity, m/s$^2$, and $\Delta\rho$ is the difference between the saturated liquid density and saturated vapor density $\Delta\rho = \rho_f - \rho_g$, kg/m$^3$ (El-Genk et al., 1988). The density ratio $\rho_g/\rho_f$ reflects the effect of the pressure and was hereby used to develop the correlation (Chang and Yao, 1983; Kim et al., 2000; Chun et al., 2001b). The channel geometry is reflected by the dimensionless diameter and the dimensionless gap size. The dimensionless diameter $D^*$ is defined by $D^* = 2D_{j_1}/(D_i + D_o)$ where $j_1$=i,o and the dimensionless gap size is given by $s^* = (D_o - D_i)/(D_o + D_i)$. The dimensionless heat flux on the other side tube is given by $q^* = 2q/(q + q_c)$.

As discussed above, supposing that the CHF is in the derivation of power equation of the general form:

$$q_{cm}^* = CG^{*a}\left(\frac{\rho_g}{\rho_f}\right)^b X_C^c\left(\frac{2D_m}{D_o + D_i}\right)^d\left(\frac{D_o - D_i}{D_o + D_i}\right)^e\left(\frac{2q_n}{q_i + q_o}\right)^f \tag{5}$$

where $m$ = i and $n$ = o for the CHF occurring on the inside tube while $m$ = o and $n$ = i for the CHF occurring on the outside tube.

Eq. (5) is transformed by taking its logarithm to yield the following equation:

$$\log q_{cm}^* = \log C + a\log G^* + b\log\left(\frac{\rho_g}{\rho_f}\right) + c\log X_C + d\log\left(\frac{2D_m}{D_o + D_i}\right) + e\log\left(\frac{D_o - D_i}{D_o + D_i}\right) + f\log\left(\frac{2q_n}{q_i + q_o}\right) \tag{6}$$

Thus, the results of the multi-variant linear regression analysis (Xu, 1995) are listed as following:

$$\frac{q_{CHF,i}}{h_{fg}\sqrt{\lambda\rho_g g\Delta\rho}} = 1.01 \times \left(\frac{G}{\sqrt{\lambda\rho_g g\Delta\rho}}\right)^{-0.153}\left(\frac{\rho_g}{\rho_f}\right)^{-0.258} \times X_C^{-0.623}\left(\frac{2D_i}{D_i + D_o}\right)^{16.4}\left(\frac{D_o - D_i}{D_o + D_i}\right)^{2.55}\left(\frac{2q_o}{q_i + q_o}\right)^{0.858} \tag{7a}$$

for the inside tube

$$\frac{q_{CHF,o}}{h_{fg}\sqrt{\lambda\rho_g g\Delta\rho}} = 0.0144 \times \left(\frac{G}{\sqrt{\lambda\rho_g g\Delta\rho}}\right)^{-0.0648}\left(\frac{\rho_g}{\rho_f}\right)^{-0.165} \times X_C^{0.0113}\left(\frac{2D_o}{D_i + D_o}\right)^{-10.1}\left(\frac{D_o - D_i}{D_o + D_i}\right)^{0.839}\left(\frac{2q_i}{q_i + q_o}\right)^{-0.436} \tag{7b}$$

for the outside tube. The relative error in Eq. (7) is defined by

$$\varepsilon = \frac{q_{EXP} - q_{CAL}}{q_{EXP}} \times 100\% \tag{8}$$

where $q_{EXP}$ is the experimental CHF and $q_{CAL}$ is the CHF obtained by Eqs. (7a) or (7b). The relative errors of Eqs. (7a) and (7b) are below ±15%.

## 6. Conclusions

Experimental study on CHF with the annular gap sizes of 0.95 and 1.5 mm in vertical narrow annuli with bilateral heating has been carried out on conditions of low pressure and low flow. The main findings are as follows.

A criterion of the appearance of dryout type CHF for bilaterally heated annuli has been presented. It depends on the heat flux ratio between the outside and inside tubes surfaces and the CHF tends to occur on the outside tube than on the inside tube on the same conditions.

The CHF occurring on the surface of inside tube has a maximum value under the pressure of 2.3 MPa while it occurring on the surface of outside tube increases with the increase of pressure. The CHFs occurring on both sides of tubes increase monotonically with the increase of mass flow velocity. However, the CHF occurring on the inside tube increases with the mass flow velocity slightly while it occurring on the outside tube increases with the mass flow velocity remarkably. The CHFs occurring on both sides of tubes increase with annular gap size, decrease with critical quality and with the other side tube wall heat flux.

Empirical correlations were developed to predict CHF in bilaterally heated annuli with influencing factors fully considered such as pressure, mass flow velocity, critical quality, channel geometry, gap size and the other wall heat flux, and they agree well with the experimental data.

## Acknowledgements

This work is financially supported by the Nuclear Power Institute of China and Program for New Century Excellent Talents in University (NCET-06-0837), to which the authors would like to express their gratitude.

## References

Becker, K.M., Letzter, A., 1975. Burnout measurements for flow of water in annulus with two-sided heating. European Two-Phase Flow Group Meeting, Haifa, Israel.
Chang, Y., Yao, S.C., 1983. Critical heat flux of narrow vertical annuli with closed bottoms. J. Heat Transfer 105, 192–195.
Chun, S.Y., Chung, H.J., Moon, S.K., 2001a. Critical heat flux under zero flow conditions in vertical annulus with uniformly and non-uniformly heated sections. Nucl. Eng. Des. 205, 265–279.
Chun, S.Y., Chung, H.J., Moon, S.K., 2001b. Effect of pressure on critical heat flux in uniformly heated vertical annulus under low flow conditions. Nucl. Eng. Des. 203, 159–174.
Chun, S.Y., Moon, S.K., Chung, H.J., 1999. Critical heat flux in non-uniformly heated vertical annulus under a wide range of pressures, multiphase flow and heat transfer. In: Proc. 4th Int. Symp. Xi'an China, pp. 380–387.
Doerffer, S., Groeneveld, D.C., Cheng, S.C., 1997. A comparison of critical heat flux in tubes and bilaterally heated annuli. Nucl. Eng. Des. 177, 105–120.
El-Genk, M.S., Haynes, S.J., Kim, S.H., 1988. Experimental studies of critical heat flux for low flow of water in vertical annuli at near atmospheric pressure. Int. J. Heat Mass Transfer 31, 2291–2304.
El-Genk, M.S., Rao, D., 1991. On the prediction of critical heat flux in rod bundles at low pressure conditions. Heat Transfer Eng. 12–4, 48–57.
Inoue, A., Lee, S.R., 1999. Influence of two-phase flow characteristics on critical heat flux in low pressure. Exp. Therm. Fluid Sci. 19, 172–181.
Jensen, M.K., Cooper, P.E., Bergles, A.E., 1976. Boiling heat transfer and dryout in restricted annular geometries. In: AICHE Symp., 16th National Heat Transfer Conference, vol. 14, pp. 205–214.
Kim, D.H., Lee, Y.H., Chang, S.H., 2007. Effects of mechanical vibration on critical heat flux in vertical annulus tube. Nucl. Eng. Des. 237, 982–987.
Kim, S.H., Baek, W.P., Chang, S.H., 2000. Measurement of critical heat flux for narrow annuli submerged in saturated water. Nucl. Eng. Des. 199, 41–48.

Kline, S.J., McClintock, F.A., 1953. Describing uncertainties in single-sample experiments. Mech. Eng. 75, 3–12.
Kirillov, P.L., Smogalev, I.P., 1969. Calculating the heat exchange crisis for a vapour–liquid mixture on the basis of a droplet-diffusion model. Report No. FEI-181, Institute of Physics and Power, Obninsk, USSR.
Kirillov, P.L., Smogalev, I.P., 1972. Calculation of heat-transfer crisis for annular two-phase flow of a steam–liquid mixture through an annular channel. Translation of Report FEI-297 of the Physics and Power-Engineering Institute, Obninsk, USSR, 1972, as Report AECL-4752 of Chalk River Laboratories, 1974.
Knudsen, J.G., Katz, D.L., 1958. Fluid Dynamics and Heat Transfer. McGraw-Hill, New York. pp. 186–195.
Lee, K.L., Bang, I.C., Chang, S.H., 2008. The characteristics and visualization of critical heat flux of R-134a flowing in a vertical annular geometry with spacer grids. Int. J. Heat Mass Transfer 51, 91–103.
Mishima, K., Nishihara, H., 1987. Effect of channel geometry on critical heat flux for low pressure water. Int. J. Heat Mass Transfer 30, 1169–1182.
Monde, M., Mitsutake, Y., Hayasi, M., 1999. Critical heat flux during natural circulation boiling on uniformly heated outer tube in vertical annular tubes submerged in saturated liquid (change in critical heat flux characteristics due to heated equivalent diameter). Int. J. Heat Mass Transfer 42, 3189–3194.
Park, J.W., Baek, W.P., Chang, S.H., 1997. Critical heat flux and flow pattern for water flow in annular geometry. Nucl. Eng. Des. 172, 137–155.
Roger, J.T., Sakudean, M., Tahir, A., 1982. Flow boiling critical heat fluxes for water in a vertical annulus at low pressure and velocities. In: 7th Int. Heat Transfer Conf., vol. 4, pp. 339–344.
Saito, T., Hughes, E.D., Carbon, M.W., 1978. Multi-fluid modelling of annular two-phase flow. Nucl. Eng. Des. 50, 225–271.
Stoddard, R.M., Blasick, A.M., Ghiaasiaan, S.M., Abdel-Khalik, S.I., Jeter, S.M., Dowling, M.F., 2002. Onset of flow instability and critical heat flux in thin horizontal annuli. Exp. Therm Fluid Sci. 26, 1–14.
Su, G.H., Gou, J.L., Fukuda, K., Jia, D.N., 2003a. A theoretical model of annular upward flow in a vertical annulus gap. Nucl. Sci. Technol. 40, 1–11.
Su, G.H., Gou, J.L., Qiu, S.Z., 2003b. Theoretical calculation of annular upward flow in a narrow annuli with bilateral heating. Nucl. Eng. Des. 225, 219–247.
Wallis, G.B., 1969. One Dimensional Two-Phase Flow. McGraw-Hill. pp. 285–286.
Wang, B.X., Zhang, J.T., Peng, X.F., 2000. Experiment study on the dryout heat flux of falling liquid film. Heat Mass Transfer 43, 1897–1903.
Xu, S.L., 1995. Common Algorithms Collection. Tsinghua University Press. pp. 372–376.